Available online at www.sciencedirect.com
ScienceDirect
International Journal of Heat and Fluid Flow 27 (2006) 821–830
International Journal of HEAT AND FLUID FLOW
www.elsevier.com/locate/ijhff

# A stress–strain lag Eddy viscosity model for unsteady mean flow

A.J. Revell [a,*], S. Benhamadouche [a,b], T. Craft [a], D. Laurence [a,b]

[a] University of Manchester, School of Manchester, P.O. Box 88, Manchester M60 1QD, UK
[b] EDF-DER-LNH, 6 quai Watier, 78401 Chatou, France

Received 7 October 2005; received in revised form 10 February 2006; accepted 4 March 2006
Available online 11 July 2006

**Abstract**

A new Eddy viscosity model is proposed to include stress–strain lag effects in the modelling of unsteady mean flows. A transport equation for the lag parameter, hereby denoted $C_{as}$, is derived from a full Reynolds stress model (RSM), to be solved in conjunction with a standard two equation Eddy viscosity model (EVM). The performance of the new $k$–$\varepsilon$–$C_{as}$ model is assessed by applying it to the flow in a homogeneous irrotational cyclic strain; a channel flow driven by a pressure gradient oscillating around a non-zero mean, and a NACA0012 profile in deep stall. For the oscillating channel, results are compared with recent large Eddy simulations (LES) of the same flow and the addition of the lag parameter equation is shown to give improved results when compared to the standard EVM outside the near wall region.


*Keywords:* URANS; EVM; Oscillating channel; Stress–strain alignment

## 1. Introduction

Many everyday turbulent flows are inherently unsteady, both industrial (e.g. flows in the cylinders of internal combustion engines, in tubines, wakes of bluff bodies, etc.) and natural (e.g. the blood flow in arteries). The unsteadiness can be a result of imposed fluctuating boundary conditions, or geometry induced oscillations, or a combination of both. The presence of such unsteadiness in a flow can significantly alter the behaviour of important parameters such as the Reynolds stresses, turbulent kinetic energy and dissipation rate. Despite the existence and development of significantly more complex and advanced modelling strategies, most industrial unsteady flows are still computed with Eddy viscosity models within an unsteady Reynolds averaged Navier–Stokes URANS framework. However, the accuracy of standard Eddy viscosity models has not been carefully established in such applications and several fundamental assumptions in their derivations for steady flows in near turbulent equilibrium no longer hold in cases.

From the work by Boussinesq (1877), the EVM provides a direct link between the turbulent stress tensor $\overline{u_i u_j}$ in its dimensionless form ($a_{ij}$, shown in Eq. (1)), where $k$ is the turbulent kinetic energy and $\delta_{ij}$ is the Kronecker delta function, and the mean rate-of-strain tensor $S_{ij}$, erroneously forcing them to be directly in phase:

$$a_{ij} = \frac{\overline{u_i u_j}}{k} - \frac{2}{3}\delta_{ij}, \quad S_{ij} = \frac{1}{2}\left(\frac{\partial U_i}{\partial x_j} + \frac{\partial U_j}{\partial x_i}\right). \tag{1}$$

The phase lag between the stress and strain tensors is essential in the case when the flow is subjected to periodic strain of relatively high frequency and the lack of this feature leads to continuous over-generation of turbulent kinetic energy (Hadžić et al., 2001). It is well documented that standard linear EVMs significantly overpredict the production of turbulent kinetic energy in the presence of strong strain. This has led to proposals for various limiters as in the $v^2$–$f$ model (Durbin, 1991), the $k$–$\omega$ SST model (Menter, 1992) and the linear production model (Guimet and Laurence, 2002) among others. The need for such

* Corresponding author.
*E-mail address:* alistair.revell@postgrad.manchester.ac.uk (A.J. Revell).

0142-727X/$ - see front matter © 2006 Elsevier Inc. All rights reserved.
doi:10.1016/j.ijheatfluidflow.2006.03.027

bounds comes from the fact that linear EVMs yield a production, $P_k$, proportional to the square of the strain rate $S_{ij}$. In contrast, a full Reynolds stress model calculates an exact production which is linear in the strain rate. Indeed, one can write exactly $P_k = C_{\text{as}} k \|S\|$ where $C_{\text{as}}$ is a non-dimensional parameter representing the degree of alignment between stresses and strains:

$$C_{\text{as}} = -\frac{a_{ij} S_{ij}}{\|S\|}. \tag{2}$$

Basara and Jakirlić (2003) solved the full stress transport equations to include the stresses in $P_k$, as a means of improving $k$ levels used in a EVM representation of the stresses subsequently applied in the momentum equation. The results show some good improvements for a range of testcases, but the computational cost is very high.

Reynolds stress models have been shown to act in some ways like an LES subgrid scale model in some inherently transient flows where they allow large-scale unsteady structures to develop in the flow, see e.g. Benhamadouche and Laurence (2003). In homogeneous cyclic strains, an RSM allows the turbulent intensity to grow until inertial effects are large enough such that the stress tensor no longer follows the strain tensor, causing turbulence production to be blocked as shown in Hadžić et al. (2001). The use of a full RSM in combination with LES might, therefore, be appealing for hybrid approaches (e.g. DES from Spalart et al., 1997), but is still often perceived as impractical for industrial applications. It is interesting to also note that the reduction of the Eddy viscosity coefficient in two equation modelling, as in Hoarau et al. (2002), calibrated on the basis of Reynolds stress modelling, can lead to the appearance of unsteady vortex structures in agreement with the physical experiment.

The aim of this work is therefore to develop a model for the stress–strain lag, $C_{\text{as}}$, which appears to be a key parameter in rapidly evolving flows. A transport equation is developed for $C_{\text{as}}$, based on the use of an RSM for the time derivative of the tensor $a_{ij}$ as well as terms including the rate of change of the strain tensor $S_{ij}$. The model will be derived and validated for homogeneous shear and channel flows, before being applied to a homogeneous cyclic strain case, an oscillating channel flow and a flow around a NACA0012 profile in deep stall. Its performance will be compared to LES results for the flow in a channel driven by a pressure gradient oscillating around a non-zero mean. LES calculations of this flow are computed and compared to recent simulations with the same parameters (see Scotti and Piomelli, 2001a,b). The objective is to use the LES database for the validation of URANS models in the future, but the current paper is limited to an introduction of this work.

## 2. Stress–strain lag

Both the stress anisotropy, $a_{ij}$, and strain rate, $S_{ij}$, are $3 \times 3$ symmetrical tensors. This is important since it can be shown that the eigenvectors of a symmetric tensor are real and orthogonal. The anisotropy tensor has zero trace ($a_{ij}\delta_{ij} = 0$) and is dimensionless by definition, whereas the strain rate tensor is an inverse time scale and has zero trace only in the condition of incompressibility, which is assumed for this work. As previously stated, the Eddy viscosity model assumes that these two tensors are aligned. DNS data from a channel flow and from homogeneous shear flow can be used to see that even in these cases, this assumption is not true.

Measuring the alignment of two $2 \times 2$ symmetric tensors is trivial since there is only one angle between the sets of orthogonal principle axes. This is important as it implies that the alignment for all two-dimensional flows is representable by a single dimensionless scalar. For a $3 \times 3$ tensor, the orientation is defined by the three Euler angles, which can be obtained through calculation of the eigenvectors. The orientation of each tensor allows the misalignment to be given as the difference between each Euler angle, and so three scalar values are necessary to define the full stress–strain lag in a fully three-dimensional flow.

The calculation of the eigenvalues of both tensors, per node, per timestep, is too expensive for large calculations. A simpler approach would be instead to consider the inner product of the two original tensors, to give a scalar measure of alignment rather than an angle. This parameter

$$C'_{\text{as}} = \frac{a_{ij} S_{ij}}{\|a\| \|S\|} = -\frac{C_{\text{as}}}{\|a\|}, \tag{3}$$

where the invariants are defined as

$$\|a\| = \sqrt{a_{ij} a_{ij}} \quad \text{and} \quad \|S\| = \sqrt{2 S_{ij} S_{ij}} \tag{4}$$

will return a value of 1 when $a_{ij}$ is aligned with $S_{ij}$ and their eigenvectors have equal signs, and a value of 0 when, for instance, there is a lag angle of 45°. The alignment parameter is intended to be employed within a two-equation modelling framework and so the term $C_{\text{as}}$ defined in Eq. (2) will, in fact, be modelled, which is limited by $\pm\|a\|$. The case $C_{\text{as}} = \|a\|$ corresponds to the result that would be returned by a linear EVM, so in effect this parameter quantifies the degree of non-linearity of the stress–strain relationship.

## 3. Derivation of the $k$–$\varepsilon$–$C_{\text{as}}$ model

The transport equation for $C_{\text{as}}$ will now be derived. This is necessary in order to capture the effects of stress–strain lag in transient flows. The aim is to correct $\nu_t$ in highly non-equilibrium flows, whilst not affecting the original EVM results in flows close to equilibrium. Given the definition of $C_{\text{as}}$ from Eq. (2), its derivative can be obtained using the product rule (where $\mathrm{D}\phi/\mathrm{D}t = \partial\phi/\partial t + U_k \partial\phi/\partial x_k$):

$$\frac{\mathrm{D}C_{\text{as}}}{\mathrm{D}t} = -\frac{1}{\|S\|}\left( S_{ij}\frac{\mathrm{D}a_{ij}}{\mathrm{D}t} + a_{ij}\frac{\mathrm{D}S_{ij}}{\mathrm{D}t} + C_{\text{as}}\frac{\mathrm{D}\|S\|}{\mathrm{D}t}\right). \tag{5}$$

It is proposed that the total derivative for $a_{ij}$ in Eq. (5) can be calculated from a full Reynolds stress model:

$$\frac{\mathrm{D}\overline{u_i u_j}}{\mathrm{D}t} = P_{ij} + \Pi_{ij} - \varepsilon_{ij} + \mathrm{Diff}_{ij}^{\mathrm{viscous}} + \mathrm{Diff}_{ij}^{\mathrm{turbulent}}. \tag{6}$$

The terms for production $P_{ij}$ and viscous diffusion, $\mathrm{Diff}_{ij}^{\mathrm{viscous}}$ are exact, but the remaining terms must be modelled. The production can be rewritten as

$$P_{ij} = -k\left(\frac{4}{3}S_{ij} + a_{ik}S_{kj} + S_{ik}a_{kj} + a_{ik}\Omega_{kj} + \Omega_{ik}a_{jk}\right), \tag{7}$$

where

$$\Omega_{ij} = \frac{1}{2}\left(\frac{\partial U_i}{\partial x_j} - \frac{\partial U_j}{\partial x_i}\right) \tag{8}$$

allowing the influence of the rotation tensor $\Omega_{ij}$ to be seen.

The tensorial dissipation in the RSM can be linked to the dissipation equation by assuming local isotropy $\varepsilon_{ij} = \frac{2}{3}\varepsilon\delta_{ij}$. This is generally assumed to be accurate as long as the Reynolds number is high. However, when the Reynolds number is lower or when approaching a wall, this is not exact. The pressure strain term $\Pi_{ij}$ will here be approximated using the SSG model of Speziale et al. (1991):

$$\begin{aligned}\Pi_{ij} = &-(C_1\varepsilon + C_1^* P_k)a_{ij} - C_2\varepsilon\left(a_{ik}a_{kj} - \frac{1}{3}\delta_{ij}A_2\right)\\ &+ (C_3 - C_3^*\sqrt{A_2})kS_{ij} + C_4 k\left(a_{ik}S_{jk} + a_{jk}S_{ik} - \frac{2}{3}a_{lm}S_{lm}\delta_{ij}\right)\\ &+ C_5 k\left(a_{ik}\Omega_{jk} + a_{jk}\Omega_{ik}\right),\end{aligned} \tag{9}$$

where the coefficients are given in Table 1.

Using the definition of the anisotropy tensor Eq. (1) the transport equation for the $a_{ij}$ can be obtained from Eq. (6), and can be written as

$$\frac{\mathrm{D}a_{ij}}{\mathrm{D}t} = \frac{1}{k}\left[P_{ij} + \Pi_{ij} - \varepsilon_{ij} - (P_k - \varepsilon)\left(a_{ij} + \frac{2}{3}\delta_{ij}\right)\right] + \mathrm{Diff}^{a_{ij}}, \tag{10}$$

where $\mathrm{Diff}^{a_{ij}}$ contains all required diffusion terms.

Rodi developed the Algebraic stress model (ASM), in which the neglection of transport of $a_{ij}$ is referred to as the weak equilibrium assumption ($\mathrm{D}a_{ij}/\mathrm{D}t - \mathrm{Diff}^{a_{ij}} = 0$) (see Rodi, 1975, 1976). This allows one to construct an algebraic approximation for the anisotropies, based on a specific RSM . In this case the anisotropy relation is implicit and a coupled, non-linear system of equations must be solved. The approach was shown to retain some features from RSMs but numerical difficulties resulting from a lack of diffusion or viscous damping lead to problems particularly for complex flows. An alternative approach, known as Explicit Algebraic Reynolds stress models (e.g. Wallin and Johansson, 2000) instead aims to obtain the anisotropy tensor explicitly in terms of the mean flow field. Some of these schemes have been shown to be accurate in rotating and sheared flows, although they remain unable to incorporate history and evolution effects of the stresses into their predictions.

The present approach is different from the ASM approach in that the entire RHS of Eq. (6) is used. Given that these terms are balanced to give the advection of the stresses, this approach will be inherently able to incorporate evolution effects. To simplify the implementation, the exact diffusion terms from the RSM will be dropped, and their effect incorporated within a simple gradient diffusion term in the general transport equation of $C_{\mathrm{as}}$. The general transport equation for $C_{\mathrm{as}}$ can therefore be rewritten, after substitution of Eq. (6) into Eq. (5) as shown below:

$$\begin{aligned}\frac{\mathrm{D}C_{\mathrm{as}}}{\mathrm{D}t} = &-\frac{1}{\|S\|}(S_{ij}P_{ij} + S_{ij}\Pi_{ij} + a_{ij}S_{ij} - a_{ij}S_{ij}\varepsilon)\\ &-\frac{1}{\|S\|}\left(a_{ij}\frac{\mathrm{D}S_{ij}}{\mathrm{D}t} + C_{\mathrm{as}}\frac{D\|S\|}{\mathrm{D}t}\right) + \mathrm{Diff}^{C_{\mathrm{as}}}.\end{aligned} \tag{11}$$

After substituting for $\Pi_{ij}$, the full transport equation for $C_{\mathrm{as}}$ for any linear or quasi-linear pressure strain model can be written as

$$\begin{aligned}\frac{\mathrm{D}C_{\mathrm{as}}}{\mathrm{D}t} = &\alpha_1\frac{\varepsilon}{k}C_{\mathrm{as}} + \alpha_1^*\|S\|C_{\mathrm{as}}^2\\ &-\alpha_2\frac{S_{ij}a_{ik}a_{kj}}{\eta}\left(\alpha_3 + \alpha_3^*\sqrt{A_2}\right)\|S\|\\ &+\alpha_4\frac{S_{ij}a_{ik}S_{jk}}{\|S\|} + \alpha_5\frac{S_{ij}a_{ik}\Omega_{jk}}{\|S\|} - \frac{1}{\|S\|}\frac{\mathrm{D}S_{ij}}{\mathrm{D}t}\\ &\times\left(a_{ij} + \frac{2C_{\mathrm{as}}S_{ij}}{\|S\|}\right) + \mathrm{Diff}^{C_{\mathrm{as}}},\end{aligned} \tag{12}$$

where

$$\begin{aligned}&\alpha_1 = (1 - C_1), \quad \alpha_1^* = -\left(1 + C_1^*\right), \quad \alpha_2 = C_2,\\ &\alpha_3 = \frac{\left(\frac{4}{3} - C_3\right)}{2}, \quad \alpha_3^* = \frac{C_3^*}{2},\\ &\alpha_4 = 2(1 - C_4), \quad \alpha_5 = 2(1 - C_5)\end{aligned}$$

and the corresponding constants for the SSG and LRR (Launder et al., 1975) pressure–strain model are given in Table 2.

The turbulent viscosity $\nu_{\mathrm{t}}$ is now taken as

$$\nu_{\mathrm{t}}^{\mathrm{new}} = k\min\left[\frac{C_\mu k}{\varepsilon}, \frac{C_{\mathrm{as}}}{\|S\|}\right] \tag{13}$$

which is derived from equating the production term for a standard EVM approach, $P_k = \nu_{\mathrm{t}}\|S\|^2$ with the new defini-

Table 1
Coefficients in the SSG pressure–strain model

| $C_1$ | $C_1^*$ | $C_2$ | $C_3$ | $C_3^*$ | $C_4$ | $C_5$ |
|---|---|---|---|---|---|---|
| 1.7 | 0.90 | 1.05 | 0.8 | 0.65 | 0.625 | 0.2 |

Table 2
Constants in the SSG and LRR pressure strain models

| | $\alpha_1$ | $\alpha_1^*$ | $\alpha_2$ | $\alpha_3$ | $\alpha_3^*$ | $\alpha_4$ | $\alpha_5$ |
|---|---|---|---|---|---|---|---|
| SSG | −0.70 | −1.90 | 1.05 | 0.267 | 0.325 | 0.75 | 1.60 |
| LRR (QI) | −0.80 | 0 | 0 | 0.267 | 0 | 0.254 | 0.69 |

tion, $P_k = C_{as} k \|S\|$ and rearranging for $\nu_t$. This appears to be a limiter similar in style to that in the SST model, although several works have developed similar approaches whereby the lower of either the turbulent or the mean flow timescales are selected to limit over-prediction of turbulent viscosity. However, the present approach not only allows viscosity to be limited in regions of high strain, but also, crucially, responds to local changes in the stress–strain alignment parameter $C_{as}$.

Finally, the diffusion term in Eq. (12) is modelled by a simple gradient-diffusion scheme:

$$\mathrm{Diff}^{C_{as}} = \frac{\partial}{\partial x_j}\left[\left(\nu + \frac{\nu_t}{\sigma_{cas}}\right)\frac{\partial C_{as}}{\partial x_j}\right] \tag{14}$$

with the constant $\sigma_{cas} = 5$.

If the model is to reproduce the log-layer region correctly, then it is a requirement that it returns the standard value of $C_\mu$ in equilibrium conditions (i.e. when the production to dissipation ratio is unity and $\eta = (k/\varepsilon)\|S\| = 3.333$). This is tested by taking Eq. (12), setting all time derivatives to zero, and neglecting convection and diffusion. Since for the linear EVM there is no normal anisotropy, $a_{ii} = 0$, it became necessary to reduce $C_3^*$ by a factor of two in order to achieve the correct balance, giving a value $C_{as} = 0.32$ which is equivalent to $C_\mu = C_{as}/\eta = 0.096$ and hence close to the standard value. If a non-linear EVM were to be employed to estimate the stresses, modification to the underlying stress transport model coefficients might not be needed, since a better representation of the normal stresses would be obtained than when adopting a linear EVM. However, for the results presented in this paper, the low Reynolds number $k$–$\varepsilon$ model proposed by Launder and Sharma (1974) is used as the baseline model, with the straightforward extension described in Eqs. (12) and (13).

A realisability bound is also imposed on $C_{as}$ in Eq. (13) by noting that the eigenvalues of $\overline{u_i u_j}$ are bounded between zero and $2k$. Imposing this lower bound on the linear EVM gives the constraint $2\nu_t \lambda^S_{max} \leqslant 2/3k$, where $\lambda^S_{max}$ is the maximum eigenvalue of the strain tensor (Durbin, 1996). Since $\lambda^S_{max} < \sqrt{\|S\|^2/3}$, the realisability of turbulent viscosity can be ensured by maintaining $\nu_t \leqslant k/\sqrt{3}\|S\|$, which leads to the inferred bound on $C_{as}$ of

$$|C_{as}| \leqslant \frac{1}{\sqrt{3}}. \tag{15}$$

## 4. Near wall treatment

At a solid boundary, $C_{as}$ is set to be zero which is the appropriate condition since in a channel flow $C_{as}$ is equal to $a_{12}$ which itself becomes zero at the wall. The transport equation for $C_{as}$ (Eq. (12)) is derived from a high Reynolds number pressure strain model (Eq. (9)), which requires special treatment as the wall is approached. In this region the quasi-homogeneous approximation for pressure strain fails (Durbin and Pettersson-Reif, 2001). A priori DNS studies show that in general the model has problems in the region $y^+ \leqslant 100$, where the non-dimensional wall units are defined as $y^+ = yU_\tau/\nu$, with $U_\tau$ the friction velocity. In the present work, the damping function

$$f^{C_{as}} = \tanh\left[\exp\left(\frac{y^+ - 80}{10}\right)\right] \tag{16}$$

is applied to all the source terms of Eq. (12) to improve near wall prediction. This function was calibrated with respect to channel flows at several different Reynolds numbers. Future development could address this issue by incorporating a low Reynolds number pressure strain model, although many of these employ damping functions dependent on near wall distance. One model that does not require the wall distance is the two component limit model of Craft (2002), and this might perhaps be an appropriate choice.

Although the above damping is required in the $C_{as}$ equation, the overprediction of $C_{as}$ in the near wall region that would result from not including it does not largely affect the results presented here. This is because close to the wall, the turbulence timescale, $k/\varepsilon$, is small compared to that associated with $C_{as}/\|S\|$ in Eq. (13).

## 5. Numerical treatment

Calculations for some of the present flows were performed using the EDF in-house CFD code, *Code_Saturne* (Archambeau et al., 2004). This is an unstructured finite-volume code based on a collocated discretization for cells of any shape. It solves turbulent Navier–Stokes equations for Newtonian incompressible flows with a fractional step method based on a prediction–correction algorithm for pressure/velocity coupling (SIMPLEC) and a Rhie and Chow interpolation to avoid pressure oscillations. A number of turbulence models are available (among them the high and low Reynolds number versions of $k$–$\varepsilon$, SSG, $v^2$–$f$, LES). Several LES calculations have been recently computed successfully with *Code_Saturne*, see e.g. Jarrin et al. (2005), Benhamadouche et al. (2002). Both the standard Smagorinsky model with a constant of 0.065 and the classical dynamic model have been used to compute the oscillating channel flow reported here. In these simulations the time advancing scheme is second order with a combination of Crank–Nicolson and Adams–Bashforth schemes, and a fully centred scheme is used for the convection term without any upwinding. In the case of non-orthogonal cells, a gradient reconstruction technique is used to maintain second order accuracy in space.

The RANS calculations of the 1D cases have been performed using a in-house one-dimensional solver.

## 6. Homogeneous irrotational cyclic strain

The evolution of turbulent kinetic energy in a general case of homogeneous turbulence subjected to a cyclic com-

pression and expansion is considered. The control volume can be thought of as being in the centre of a very large compression chamber, thus excluding secondary motions and wall effects. The imposed strains $S_{11} = 2/3S(t)$, $S_{22} = S_3 = -1/3S(t)$ to ensure continuity. The time dependent strain, $S(t)$ is taken as

$$S(t) = \frac{\omega \cos(\omega t)}{\sin(\omega t) + \frac{5}{4}} \tag{17}$$

so

$$\frac{\mathrm{d}S(t)}{\mathrm{d}t} = \omega^2 \left[ \left( \frac{\sin(\omega t)}{\sin(\omega t) + \frac{5}{4}} \right) + \left( \frac{\cos(\omega t)}{\sin(\omega t) + \frac{5}{4}} \right)^2 \right]. \tag{18}$$

In this case, $U$ is the local axial mean flow velocity, $x$ denotes piston direction and $t$ time from zero. The external parameter is the piston motion period $T$, which is used to non-dimensionalise $t$. We consider a typical internal combustion engine case with a piston stroke of $1 - 1/r = 4/5$, where $r$ is the compression ratio.

The variation of both $S(t)$ and $\mathrm{d}S(t)/\mathrm{d}t$ are shown in Fig. 1.

We now solve numerically both an EVM and an RSM for the same case of homogeneous cyclic compression. For a demonstration of the differences between these two models, it is not important which particular EVM or RSM is used, although here we present results from the standard $k$–$\varepsilon$ and SSG RSM. Results will also be shown for the $C_{\mathrm{as}}$ model.

It can be seen from Fig. 2a that when the $k$–$\varepsilon$ model is employed the turbulent kinetic energy explodes, since the production is always positive. It is also seen that the stress and strain are directly in phase, with their maxima occuring at the same phase locations. Conversely, when the RSM is used, (Fig. 2b) the kinetic energy decays, due to a net zero production averaged over each cycle, which, combined with the dissipation, causes an overall net decay. These results also indicate a phase lag of $\pi/2$ between the maxima of stress and strain, which was not captured by the $k$–$\varepsilon$ model. In this case there is a stark difference between the results from the two turbulent closure schemes, brought about by the failure of the EVM to decouple the turbulent stresses from the strains. Under homogeneous conditions the contribution of both convection and diffusion is zero, thus this difference is due in large to the representation of the production term.

The exact production rate of turbulent kinetic energy, $P_k = -\overline{u_i u_j} S_{ij}$, is the simply the trace of the stress production term in Eq. (7). However, due to the formulation of the stress–strain relation, the production term that appears with a linear EVM is equivalent to $P_k = \nu_{\mathrm{t}} \|S\|^2$. The turbulent viscosity in a two equation framework is generally always positive, since $\nu_{\mathrm{t}}$ is calculated from $k$ and either $\varepsilon$ or $\omega$, which themselves are always positive. In this way a negative production, or a back transfer of energy from turbulent motion to the mean flow, can not be achieved in a two equation context, whereas the independent calculation of turbulent stresses as in an RSM does not prevent this.

Furthermore, while one might expect an approximation of stresses from an NLEVM to correctly model the production, since more anisotropy is added, this is not always true. It is possible in some cases to obtain a negative production with an NLEVM, but exactly how much and under what strain rates depends on the exact forms adopted for the non-linear coefficients and $C_\mu$.

When the $C_{\mathrm{as}}$ model is used (Fig. 2c) the results of the RSM are almost exactly reproduced, with only a slight difference in the decay rate of $k$ and $\varepsilon$. There is clearly a phase lag present between the stress $\overline{u_1^2}$ and the strain $S_{11}$, although the stress curves do show a small kink where $S_{11} = 0$, since they are calculated using the linear EVM, so when the strains are zero, the normal stresses return to $2/3k$. The $C_{\mathrm{as}}$ model's performance in this case is largely due to the $\mathrm{D}S_{ij}/\mathrm{D}t$ term in the $C_{\mathrm{as}}$ equation, since, together with the slow pressure strain term (the first term in Eq. (12)) are the only non-zero terms when $S_{ij} = 0$. Indeed it is the change of sign of $C_{\mathrm{as}}$ which allows the production

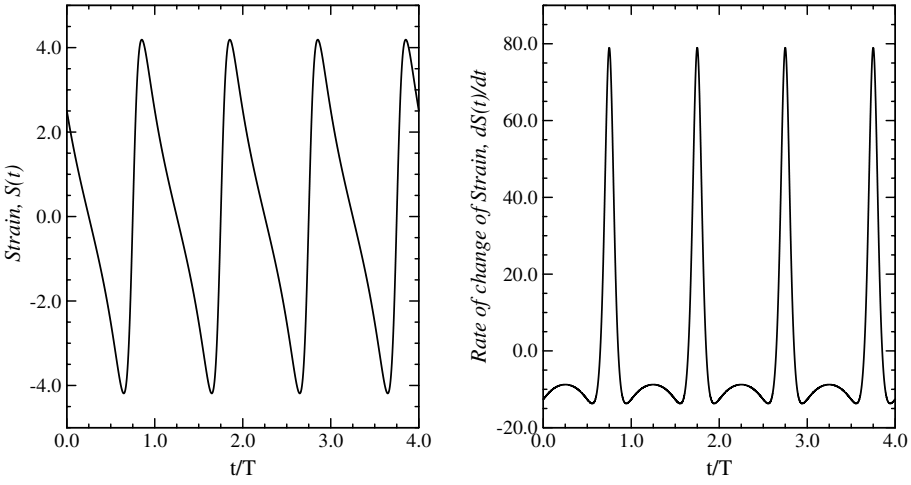


Fig. 1. Strain and rate of change of strain verses time.

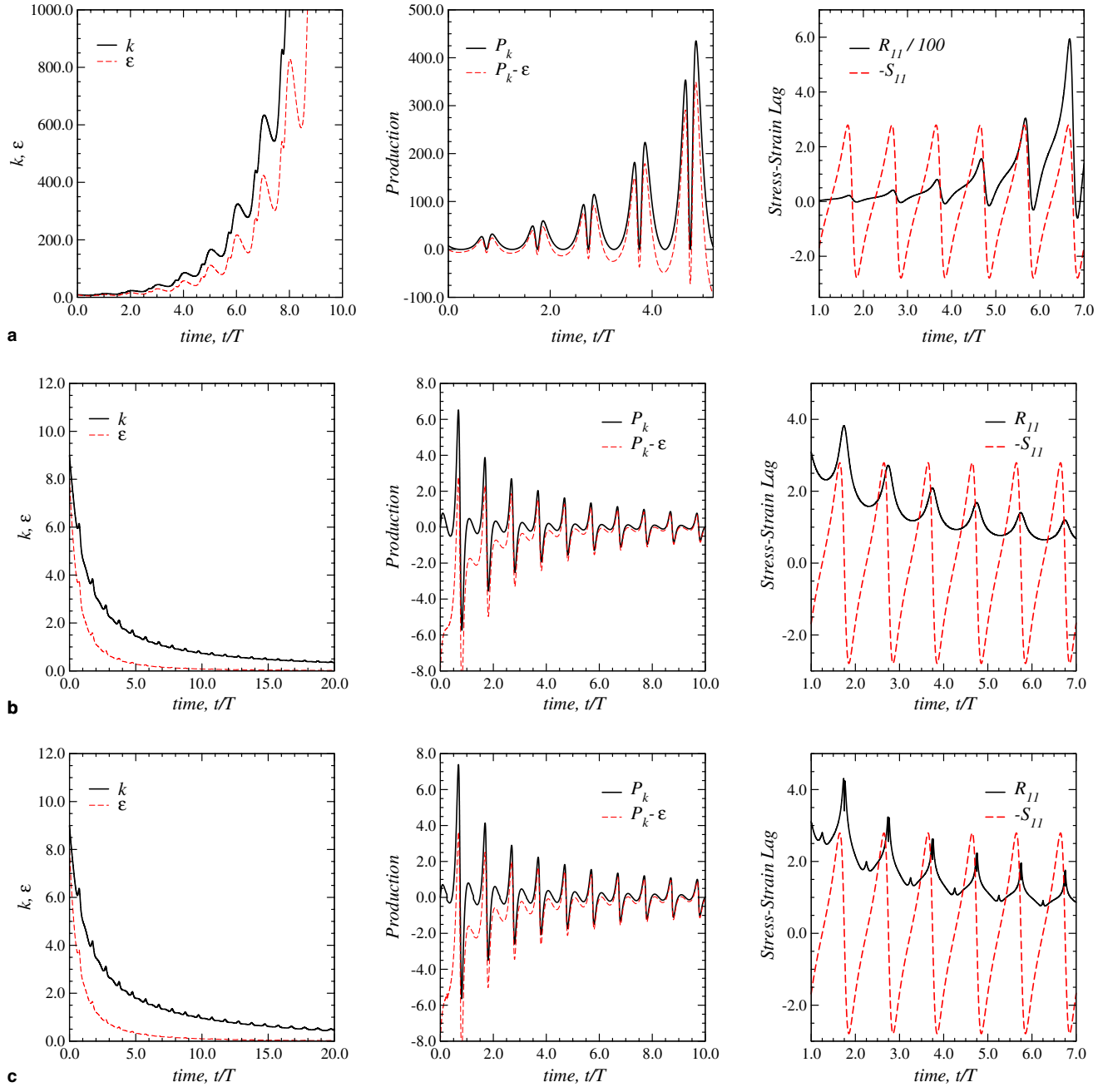


Fig. 2. Performance of models for turbulence subjected to a cyclic strain. Plots of left column: $k$ and $\varepsilon$, centre column: production of $k$ and net balance $P_k$–$\varepsilon$, right column: comparison of stress and strain. (a) Top row: standard $k$–$\varepsilon$; (b) middle row: SSG Reynolds stress model; (c) bottom row: present $k$–$\varepsilon$–$C_{as}$ model.

to become negative and therefore permit a zero contribution over one period to the source terms of the turbulence transport equations. It is important to note that in inhomogeneous flows, this term would also include the spatial convection of the strains and thus its influence is not limited solely to unsteady flows.

## 7. Oscillating channel

In this case, it was proposed to examine how the model is able to handle a wall bounded flow with imposed unsteadiness. LES results are available to describe the periodic variation of the flow field. The flow is forced by a mean pressure gradient following the notations given in Scotti and Piomelli:

$$P_f(x,t) = \Delta P_0 \left[1 + \alpha \cos\left(\Omega t + \frac{\pi}{2}\right)\right] x/L_x. \tag{19}$$

In the following, the frequency $\Omega = 3.57\ \mathrm{s}^{-1}$ and the amplitude $\alpha = 50$, which is referred to in Scotti and Piomelli as an intermediate frequency. This is an interesting frequency which causes the turbulent quantities to become out of

phase and is therefore suitable to the present study (whereas the higher frequencies influence only the flow very close to the wall). The pressure is lagged in order to start the acceleration phase at $\Omega t = 2\pi t/T$ where $T$ is the period time. The channel half height $\delta$ and the mean pressure gradient $\Delta P_0/L_x$ are set to give a Reynolds number of 350, based on the mean friction velocity $u_\tau = \sqrt{\delta \Delta P_0/2\rho L_x}$. A set of 100 nodes is used to discretize the 1D domain for the URANS calculations with a near wall refinement. As commented earlier, a further LES study of this flow was also conducted, to provide more detailed data against which to validate the present model.

The domain size in these LES calculations is $6\delta\pi \times 4\delta \times 3/2\delta\pi$ and the number of cells is $64 \times 64 \times 65$ with wall refinement. The maximum Courant number in all the calculation did not exceed 1. In all the computations, a phase averaging is used to compute mean values. Phase averaging is denoted by $\langle\cdot\rangle$. It is defined for a physical variable $\phi$ as follows:

$$\langle\phi\rangle_{\mathrm{URANS}}(y,t) = \frac{1}{N}\sum_{n=1}^{N} f\left(y, \frac{t}{T} + n\right) \tag{20}$$

$$\langle\phi\rangle_{\mathrm{LES}}(y,t) = \frac{1}{N}\sum_{n=1}^{N} \frac{1}{L_x L_y}\int_0^{L_x}\int_0^{L_z} f\left(x, y, z\frac{t}{T} + n\right)\mathrm{d}z\,\mathrm{d}x \tag{21}$$

Initial work was carried out to validate the LES for the oscillating channel flow. Fig. 3 shows the periodic variation of several quantities for the two LES models employed in the present work, Scotti and Piomelli's LES and the URANS computations. Overall the agreement between the three LES calculations is very reasonable, although the dynamic model seems to overpredict both the velocity and kinetic energy in comparison to the other two, particularly in the later acceleration and early deceleration stages (between $t/T = 0.25$ and $t/T = 0.75$). There is a slight discrepancy in the variation of the wall shear stress between the new results and the reference data, where a bump appearing between $t/T = 0.6$ and $t/T = 0.9$ is not picked up by the former. This is mirrored by discrepancies in the periodic variation of kinetic energy, for the same time bracket, which also corresponds to the deceleration region of the oscillation (between $t/T = 0.5$ and $t/T = 1$). This behaviour is an indication of the strong influence of near wall phenomena on the rest of the flow.

Although the reference profile of kinetic energy suffers from a lack of data points, the asymmetric bump during deceleration shown by all 3 LES profiles is a well documented feature of this flow and should not be ignored. The $k$–$\varepsilon$–$C_{\mathrm{as}}$ models are in very good agreement with the LES data in the acceleration phase, where $k_{\max}$ undergoes a slow increase, and the agreement with the velocity profile is also improved with respect to the standard model for the same time period. After around $t/T = 0.6$ the predicted $k_{\max}$ values start to decrease rather too early compared to the LES data. The standard $k$–$\varepsilon$ model, in contrast, does not predict an increase in $k_{\max}$ until the early deceleration period (around $t/T = 0.55$). It then predicts a very rapid increase, followed by a decrease which does broadly agree with the LES data in the later deceleration phase, from around $t/T = 0.75$. Given the fairly decent agreement between the low Reynolds number $k$–$\varepsilon$ and the reference data in this late deceleration phase, it might be concluded that the selection of a good near wall model or damping function, together with an adequate near wall refinement is enough to capture the main features of this stage of the flow. It is important to note that in the acceleration phase the Reynolds number is higher

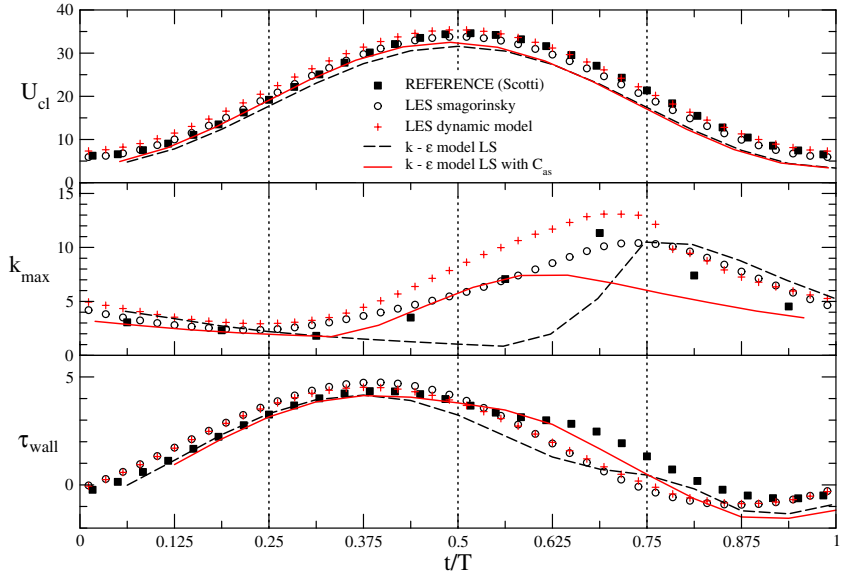


Fig. 3. Time series over period of oscillation for centreline velocity $U_{\mathrm{cl}}$, maximum streamwise kinetic energy $k_{\max}$ and wall shear stress $\tau_{\mathrm{wall}}$. Comparison to LES reference data from for validation of LES dynamic and LES Smagorinksy models. Results from low Reynolds number $k$–$\varepsilon$ model, with and without $C_{\mathrm{as}}$ modified viscosity.

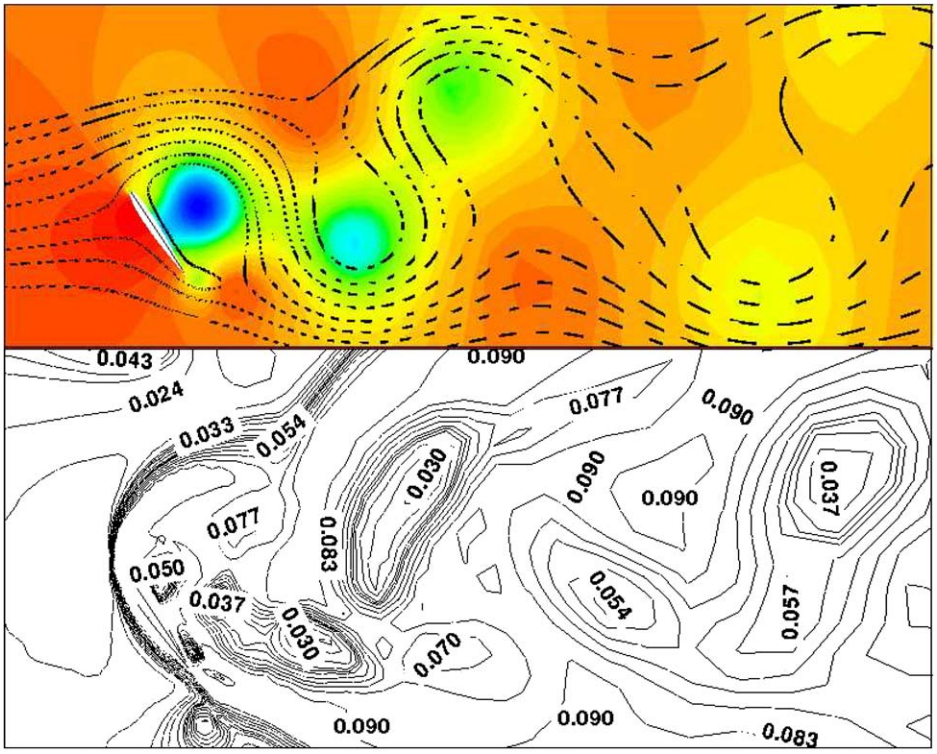


Fig. 4. Preliminary results for flow around NACA0012 at max lift at an incidence of 60° using $k$–$\varepsilon$–$C_{as}$ model. Top: Contour plot of pressure overlaid with flow streamlines. Bottom: Contour lines of modified $C_\mu$ with labels. Both at same location and time.

and so near wall effects are confined to a region closer the wall, with the opposite being true for the deceleration phase.

This flow is certainly influenced to a large extent by its near wall features and the above results show an apparent phase switch between best predictions being offered by the $k$–$\varepsilon$–$C_{as}$ model over much of the flow, although by the standard $k$–$\varepsilon$–$C_{as}$ in the later deleceration period. This is likely due to the fact that the terms of the $C_{as}$ transport equation are not valid in the near-wall viscous layer. Since they come directly from the high Reynolds SSG model, there is no damping of the pressure strain or other processes. The low Reynolds $k$–$\varepsilon$ model shows an improved behaviour in the deceleration region (where, as noted earlier, the viscous layer is thicker) and it is reasonable to expect that a low Reynolds number version of the $k$–$\varepsilon$–$C_{as}$ model would return similar improvements.

## 8. Flow around NACA0012 at high incidence

As a demonstration of the $k$–$\varepsilon$–$C_{as}$ model's applicability to more complex flows, the flow around a NACA0012 airfoil at an incidence angle of 60° has been computed. In this case the wake is massively separated and unsteady, and should therefore provide a good test for the $k$–$\varepsilon$–$C_{as}$ scheme.

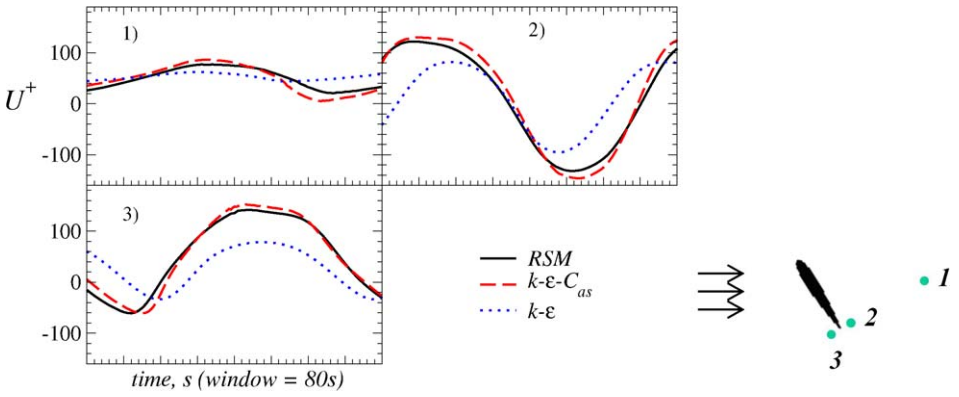


Fig. 5. Preliminary results for flow around NACA0012 at max lift at an incidence of 60°. Evolution of velocity at three probe locations around the aerofoil, compared by the SSG RSM, the $k$–$\varepsilon$ model and the $k$–$\varepsilon$–$C_{as}$ model.

Fig. 4 shows contour plots from some early calculations of this flow. It can be seen that the model captures the unsteady separation and that $C_\mu$ is reduced in regions corresponding to the shed vortex structures (shown by the pressure contours and flow streamlines). In Fig. 5 the improvements achieved by using the $C_{as}$ model relative to a standard two equation model can be seen more clearly. The model gives results that very closely mimic those obtained from a full stress transport closure. It can also be noted that the behaviour shown is in agreement with the prediction of strongly detached flows by modified two equation models (with $C_\mu$ reduced) in the context of Organised Eddy Simulation (Hoarau et al., 2002). This reduced $C_\mu$ approach has also been used to improve the RANS length scale in DES for the same NACA0012 configuration (Braza and Hoarau, submitted for publication).

## 9. Conclusions and future work

The degree of alignment of stresses and strains has been expressed as a dimensionless parameter ($C_{as}$) and a transport equation derived to account for the evolution of this quantity. The equation is derived from a full RSM model so as to incorporate phase lag information and to automatically limit the production of kinetic energy in regions of strong strain. The Eddy viscosity is globally modified, to be a function of $C_{as}$, so there is no discrepancy between that used in the turbulent transport and in the mean flow equation.

The motivation behind the model development stems from the observation that in rapidly varying mean flows, such as bluff body wakes or around staggered tube bundles, RSMs can produce large unsteady structures, whilst standard Eddy viscosity models tend to generate excessively high levels of turbulent energy, damping out such unsteadiness. In the flows examined, the model has performed well: in the case of cyclic straining and massively separated flow behind an aerofoil it produced results almost identical to those from a stress transport scheme, whilst in the oscillating channel flow the predictions were generally in good agreement with recently generated LES results. A detailed study of the model's performance in flow around a circular cylinder is now in progress (Perrin et al., 2005).

The $k$–$\varepsilon$–$C_{as}$ would appear to be an economical alternative to using a full stress transport model in some circumstances, since its computational expense and coding complexity are only slightly greater than required by typical $k$–$\varepsilon$ schemes. For more complex applications it might, however be beneficial to apply it within the context of a non-linear Eddy viscosity model, in order to obtain better stress anisotropy predictions. Elements of the model might also be adapted for use in DES applications, where its response in regions of stress–strain lag could be used to identify the transition region between different modelling approaches, where unsteadiness starts to emerge, in a more general manner to the ad-hoc switching based on grid characteristics that is commonly employed.

## Acknowledgements

Authors are grateful to A. Scotti and U. Piomelli for fast and friendly provision of their LES data and clarifications for its use. Financial support via the FLOMANIA and DESider projects is also acknowledged.

The FLOMANIA project (Flow Physics Modelling – An Integrated Approach) is a collaboration between Alenia, AEA, Bombardier, Dassault, EADS–CASA, EADS–Military Aircraft, EDF, NUMECA, DLR, FOI, IMFT, ONERA, Chalmers University, Imperial College, TU Berlin, UMIST and St. Petersburg State University. The project is funded by the European Union and administrated by the CEC, Research Directorate-General, Growth Programme, under Contract No.G4RD-CT2001-00613.

The DESider project (Detached Eddy Simulation for Industrial Aerodynamics) is a collaboration between Alenia, ANSYS–AEA, Chalmers University, CNRS–Lille, Dassault, DLR, EADS Military Aircraft, EUROCOPTER Germany, EDF, FOI–FFA, IMFT, Imperial College London, NLR, NTS, NUMECA, ONERA, TU Berlin, and UMIST. The project is funded by the European Community represented by the CEC, Research Directorate-General, in the 6th Framework Programme, under Contract No. AST3-CT-2003-502842.

This work was also aided in part by the Marie Curie Fellowship Program, contract number HPMT-CT-2000-00079.

## References

Archambeau, F., Mechitoua, N., Sakiz, M., 2004. A finite volume method for the computation of turbulent incompressible flows – industrial applications. Int. J. Fin. Vol.

Basara, B., Jakirlić, S., 2003. A new hybrid turbulence modelling strategy for industrial CFD. Int. J. Numer. Meth. Fluids 42, 89–116.

Benhamadouche, S., Laurence, D., 2003. Les, course les, and transient rans comparisons on the flow across a tube bundle. Int. J. Heat Fluid Flow 24, 470–479.

Benhamadouche, S., Mahesh, K., Constantinescu, G., 2002. Collocated finite volume schemes for less on unstructured meshes. In: CTR. Proceedings of the 2002 Summer Program, Stanford.

Boussinesq, J., 1877. Theorie de l'écoulement tourbillant. Mém. Prés. par div. savant a lacad. sci. Paris 23, 46.

Braza, M., Hoarau, Y., in press. Prediction of the unsteady 3d flow past a naca0012 wing beyond stall by DES-OES approach. In: Notes on Numerical Fluid Mechanics and Interdisciplinary Design – FLOMANIA European program, Springer.

Craft, T.J., 2002. Closure modelling near the two-component limit. In: Launder, B.E., Sandham, N. (Eds.), Closure Strategies for Turbulent and Transitional Flows. CUP, pp. 102–126.

Durbin, P., 1991. Near-wall turbulence closure modelling without 'damping functions'. Theor. Comput. Fluid Dyn. 3, 1–13.

Durbin, P.A., 1996. On the $k$-3 stagnation point anomaly. Int. J. Heat Fluid Flow 17, 89–90.

Durbin, P.A., Pettersson-Reif, B.A., 2001. Statistical Theory and Modelling for Turbulent Flows. John Wiley & Sons, Ltd.

Guimet, V., Laurence, D., 2002. In: A linearised turbulent production in the $k$–$\varepsilon$ model for engineering applications. ETMM5, Mallorca, Spain.

Hadžić, I., Hanjalić, K., Laurence, D., 2001. Modeling the response of turbulence subjected to cyclic irrotational strain. Phys. Fluids 13 (6), 1740–1747.

Hoarau, Y., Braza, M., Rodes, P., Tzabiras, G., Allain, C., Favier, D., Berton, E., Maresca, M., 2002. Turbulence modelling of unsteady flows with a pronounced periodic character around an airfoil. In: Proceedings, IUTAM symposium, Unsteady Separated Flows, Toulouse, France.

Jarrin, N., Benhamadouche, S., Laurence, D., 2005. Inflow conditions for LES using a new vortex method. TSFP4, Virginia, USA, 693–698.

Launder, B.E., Sharma, B.I., 1974. Application of the energy-dissipation model of turbulence to the calculation of flow near a spinning disk. Lett. Heat Mass Transfer 1, 131–138.

Launder, B.E., Reece, G.J., Rodi, W., 1975. Progress in the development of a Reynolds stress turbulence closure. J. Fluid Mech. 68, 537–566.

Menter, F.R., 1992. Two-equation Eddy-viscosity turbulence models for engineering applications. AIAA J. 32, 1598–1605.

Perrin, R., Braza, M., Cid, E., Cazin, S., Moradei, F., Barthet, A., Sevrain, Y., Hoarau, Y., 2005. Near-wake turbulence properties in the high reynolds incompressible flow around a circular cylinder by 2c and 3c piv. In: Proc. ETMM6 Conf., Sardinia, Ital, Sardinia, Italy.

Rodi, W., 1975. The prediction of free turbulent boundary layers by use of a two equation model of turbulence. Ph.D. thesis, University of London.

Rodi, W., 1976. A new algebraic relation for calculating the Reynolds stresses. Z. Angew. Math. Mech. 56, 219–221.

Scotti, A., Piomelli, U., 2001a. Numerical simulation of pulsating turbulent channel flow. Phys. Fluids 13 (5), 1367–1384.

Scotti, A., Piomelli, U., 2001b. Turbulence models in pulsating flows, AIAA Paper (2001-0729).

Spalart, P. R., Jou, W.-H., Strelets, M., Allmaras, S.R., 1997. In: Liu, C., Liu, Z. (Eds.), Comments on the Feasability of LES for Wings, and on a Hybrid RANS/LES Approach. First AFOSR International Conference on DNS/LES 4–8 August, Rushton, LA.

Speziale, C.G., Sarkar, S., Gatski, T.B., 1991. Modeling the pressure strain correlation of turbulence: an invariant dynamical systems approach. J. Fluid Mech. 227, 245–272.

Wallin, S., Johansson, A.V., 2000. An explicit algebraic stress model for incompressible and compressible turbulent flows. J. Fluid Mech. 403, 89–132.